ECOHYDROLOGY
Ecohydrol. (2016)
Published online in Wiley Online Library
(wileyonlinelibrary.com) DOI: 10.1002/eco.1730

Sub-annual variability in historical water source use by Mediterranean riparian trees

Christopher I. Sargeant[1]* and Michael Bliss Singer[1,2]

[1] *Department of Earth and Environmental Sciences, University of St Andrews, St Andrews, UK*
[2] *Earth Research Institute, University of California Santa Barbara, Santa Barbara, CA, USA*

ABSTRACT

The seasonal availability of water within a tree's rooting zone may be an important determinant for individual tree growth and overall forest health, particularly in riparian corridors of Mediterranean climate zones that are vulnerable to water stress. Here, we present a new method that combines dendro-isotopes and isotope modelling for determining how water source use varies over 10 consecutive growing seasons (2000–2010) for co-occurring species *Populus nigra* and *Fraxinus excelsior*, along the Rhône River, south-eastern France. We conducted highly resolved $\delta^{18}O$ analysis of cellulose micro-slices within tree-rings and back-calculated the $\delta^{18}O$ signature of source water available at the time of growth using a biochemical fractionation model. We related these patterns to inferred seasonal hydrological partitioning through comparison with $\delta^{18}O$ of waters from the vadose and phreatic zones, precipitation and streamflow. The shallowly rooted *Fraxinus* displayed greater sub-annual source water variability, as well as greater isotopic enrichment, reflecting use of precipitation-derived vadose moisture. Its earlywood was formed mainly from winter rainfall ($\delta^{18}O$ depleted) whilst the latewood was composed from growing season precipitation ($\delta^{18}O$ enriched). In *Populus*, the sub-annual source water use was relatively depleted, suggesting use of hyporheic water and regional groundwater. From 2007, both species converged in their pattern of water source uptake which was attributed to a decline in phreatic water access for *Populus*. These results demonstrate that the seasonal variability in source water use can be identified retrospectively, a method which may prove important for anticipating the future consequences of climate-driven changes to the hydrological cycle. © 2016 The Authors. *Ecohydrology* published by John Wiley & Sons, Ltd.

KEY WORDS tree-rings; cellulose; $\delta^{18}O$; riparian; phreatic; vadose; floodplain; hydrology; climate; plant–water relations

Received 28 October 2015; Revised 25 January 2016; Accepted 8 February 2016

INTRODUCTION

Climate is understood to dynamically control water availability to forest trees. The signatures of tree water use in response to climatically driven water availability are preserved within tree-ring cellulose ($\delta^{18}O$), but they are not well understood (McCarroll and Loader, 2004 and references therein). This limits scientific capability to anticipate how variability and trends in climate will control water availability at the root zone and its uptake by plants. This is particularly relevant in riparian forests, where there are strong connections between vegetation and hydrology and where trees may access various water sources based on rooting depth and climatic forcing. The susceptibility of riparian forests to changes in the availability of water within terrestrial storage reservoirs (i.e. vadose and phreatic zones) is well appreciated (Dufour and Piégay, 2008; Scott *et al.,* 2000; Singer *et al.,* 2013). Yet there is a lack of information regarding the seasonal progression of water partitioning within these floodplain reservoirs and its uptake by trees. Such seasonal variability in water source availability and water use may complicate interpretation of annual tree-ring isotopes because mean values for a particular year may not be reflective of the dominant climatic forcing (e.g. precipitation-derived soil water v. streamflow-driven phreatic water). This limitation in seasonal understanding of water-plant relations may prove problematic for anticipating or predicting climatic responses of forests in regions, such as the Mediterranean, where hydrological regimes are predicted to be strongly influenced by rising temperatures and changes to the magnitude and timing of precipitation (Kovats *et al.,* 2014).

We plan to fill this research gap by testing the utility of a novel method to elucidate the seasonal partitioning of water and its availability to trees. We aim to reconstruct the seasonal water source history used by trees for growth as a function of regional hydrology by combining tree-ring isotopic analysis at high temporal resolution with biomechanistic modelling.

*Correspondence to: Christopher I. Sargeant, Department of Earth and Environmental Sciences, University of St Andrews, Irvine Building, North Street, St Andrews KY16 9AL, UK.
E-mail: cs456@st-andrews.ac.uk

Isotope tree-ring studies can provide detailed, historical records of the ecohydrological processes occurring during the time of growth, including the source-water uptake, for riparian forests (Alstad *et al.,* 2008; Marshall and Monserud, 2006; Singer *et al.,* 2013; Singer *et al.,* 2014). This is achieved through analysis of oxygen isotope ratios within tree-ring cellulose ($\delta^{18}O_{cell}$), which preserves a signal from source water used by trees during growth. This signal is, however, modified via fractionation mechanisms arising from meteorological (evaporative enrichment) and physiological (photosynthate production) processes at the leaf level, as well as isotope exchanges during cellulose synthesis prior to fixation within the tree ring (McCarroll and Loader, 2004). Several studies have modelled the isotopic modification of $\delta^{18}O$ in water along its path from the roots to leaves and its ultimate preservation in tree-ring cellulose. Bio-mechanistic models (e.g. Barbour *et al.,* 2004; Roden *et al.,* 2000) have demonstrated successes in predicting cellulose $\delta^{18}O_{cell}$ from a known source-water signature ($\delta^{18}O_{sw}$) by accounting for the relevant environmental and physiological parameters driving the fractionation of oxygen isotopes before the incorporation into cellulose. By accurately constraining these variables it is possible to use $\delta^{18}O_{cell}$ to determine the $\delta^{18}O_{sw}$ used during the growing season (Singer *et al.,* 2014). Yet, such annual (whole-ring) analyses only provide an integrated signal of water-use over the entire growing season (Alstad *et al.,* 2008; Marshall and Monserud, 2006; Singer *et al.,* 2013; Singer *et al.,* 2014), which may belie seasonal dynamics in water availability. There is, however, additional information stored in tree rings at a sub-annual resolution that could contribute to new understanding of the details of how source-water availability may change throughout the critical growing period in response to climate fluctuations and seasonal evolution of water availability (Treydte *et al.,* 2014). Such seasonal variations in source-water uptake may exert important controls on plant and forest-level health and thus require further investigation.

Sub-annual tree-ring isotope analyses offer the potential to elucidate seasonal patterns of source-water use. This involves extracting isotopic information from tree cores at high temporal resolution through the sub-division of individual growth rings into fine segments (micro-slices). The premise is that annual growth is achieved through the successive deposition of organic matter, including cellulose, with each segment corresponding to a portion of the growing season and containing isotopic information related to the time of formation (Berkelhammer and Stott, 2009; Treydte *et al.,* 2014). Published research which focusses on the record of sub-annual variations in tree-ring isotopes is relatively limited and particularly lacking for riparian zones, where there may be interesting ecohydrological dynamics associated with variability in two potential water sources (hyporheic streamflow-driven phreatic water and precipitation-derived vadose zone water). This method has been utilized for the development of $\delta^{18}O$ chronologies in tropical tree species where distinct rings are not visible (Evans and Schrag, 2004; Managave *et al.,* 2011), to develop an understanding of paleoclimate dynamics (Berkelhammer and Stott, 2009), and in combination with $\delta^{13}C$ to constrain seasonal physiological responses (Poussart and Schrag, 2005; Verheyden *et al.,* 2004; Verheyden *et al.,* 2006). Treydte *et al.* (2014) showed through sub-annual analyses, that seasonal trends in $\delta^{18}O_{cell}$ primarily reflect the variability in $\delta^{18}O_{sw}$, presenting great promise for this method to reveal information on past climate controls over water availability.

In non-tropical biomes sub-annual tree-ring isotopes have been used to identify water availability and climatic conditions throughout the growing season. Barbour *et al.* (2002) found that sub-annual $\delta^{18}O$ values for *Pinus radiata* reflected the seasonal variations in water source use as did Sarris *et al.* (2013) with Mediterranean *Pinus halepensis* which relied on deeper moisture sources, (depleted $\delta^{18}O_{cell}$), during drought conditions. To reliably interpret highly resolved $\delta^{18}O_{cell}$ values in relation to water sources requires a clear isotopic characterization of local and regional sources of water (e.g. Nakatsuka *et al.,* 2004). Furthermore, the use of co-occurring trees with different rooting depths can bolster the interpretation of seasonal changes in source-water utilization by alluvial forests in response to climatically driven changes in hydrology because the trees integrate different water source reservoirs (e.g. Singer *et al.,* 2013).

The isotopic content ($\delta^{18}O$ and δD) of different hydrological reservoirs is governed by the fractionation history of the contributing water source, resulting from phase changes as it moves through the water cycle (Gat, 1996). This makes it possible to identify the source of water used by plants, given that no fractionation occurs during root uptake (Dawson and Ehleringer, 1991). Indeed, a body of literature exists on the use of isotope analyses of xylem water $\delta^{18}O$ (and its origin) in determining how riparian plant–water relations vary at seasonal scales (Brooks *et al.,* 2010; Busch *et al.,* 1992; Lambs *et al.,* 2002; Penna *et al.,* 2013; Sánchez-Pérez *et al.,* 2008; Snyder and Williams, 2000; Tang and Feng, 2001; Williams and Cooper, 2005). However, such studies commonly involve contemporaneous measurements and are limited by a lack of historical information describing hydrological variability in response to climate. Extending this record retrospectively is a scientific priority in order to anticipate the vulnerability of riparian forests to alterations in the hydrological regime under future climate conditions.

Riparian zones are hydrologically dynamic and receive inputs from streamflow (overbank), hyporheic, precipita-

tion and regional groundwater sources all of which vary in space and over time (Figure 1). If the isotopic signatures of such water sources are distinct, the processes of hydrological partitioning can be documented, even if water source signatures vary. Generally, vadose zone moisture is more enriched compared to phreatic water, reflecting inputs from precipitation which undergo evaporative losses from the soil (Gazis and Feng, 2004). In contrast, the phreatic zone in river floodplains is commonly derived from hyporheic discharge of depleted river water, especially in large basins draining mountainous regions, although the presence of a regional groundwater source may impart an isotopic signature indicative of the recharge zone (Gat, 1996). Climate controls the amount of water delivered to each floodplain reservoir and thus the rooting zone of riparian trees (Singer *et al.,* 2013). Yet the availability of water to riparian forests is further modified through species-specific differences in rooting morphology and the local topographic and substrate characteristics (Singer *et al.,* 2014). Fluctuations in the water delivered to each floodplain compartment can therefore have disproportionate impacts on trees of different functional types and physiology.

The susceptibility of riparian phreatophytes (which root into the saturated zone) to water table depression has been studied for certain species, e.g. *Populus spp*, with growth retardation and mortality commonly observed, as a result of reduced streamflow and/or hydraulic connectivity with the channel, which leads to a decline in phreatic water availability (Amlin and Rood, 2002; Lambs *et al.,* 2006; Rood *et al.,* 2003; Scott *et al.,* 2000; Smith *et al.,* 1991; Stromberg and Patten, 1996). For shallowly rooted species such as *Fraxinus spp*, moisture uptake is limited to the vadose zone because of mechanical impedance of root growth by gravelly substrates, the elevation of which is regarded as the upper limit of the phreatic zone (Singer *et al.,* 2013). Rooting depth is a major control on the source of water utilized and also the vulnerability of particular tree types to changes in water partitioning. Such changes can lead to modifications in population/stand dynamics where hydrological changes favour the expansion of a certain species, whilst being detrimental to another (González *et al.,* 2010). Indeed, much of the prior work in this area has focussed on the effects of hydrological changes on individual or plant community performance. Very little research exists on exploiting tree-ring isotope records to inform understanding of responses to hydrological variability. We envisage that such data could provide resource managers, including those working to restore riparian systems which have undergone human alteration, with key historical and baseline data for anticipating ecohydrological consequences of climate change (Stella *et al.,* 2012).

In this paper we assess the utility of sub-annual tree-ring $\delta^{18}O$ analyses for interpreting the historical, seasonal water use of riparian trees as a function of regional hydrology and climate. We analysed the $\delta^{18}O_{cell}$ of micro-slices from ten consecutive tree-rings of two co-occurring tree species; *Fraxinus excelsior* and *Populus nigra*. The streamside trees were sampled from along the Rhône River, southern France which is projected to experience decreased precipitation and discharge concomitant with enhanced drying during

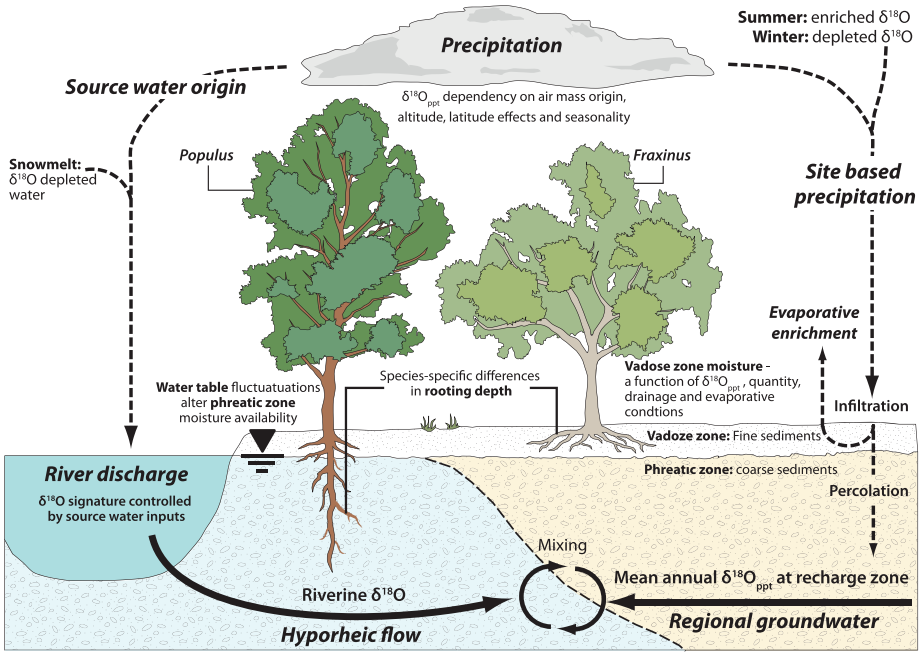

Figure 1. Conceptual diagram of isotope hydrology within the riparian zone. Common riparian species *Fraxinus excelsior* and *Populus nigra* are shown to have differing access to water sources which can be identified isotopically.

this century (Etchevers *et al.,* 2002; Boé *et al.,* 2009; Mariotti *et al.,* 2008; Jin *et al.,* 2010). We modelled the source water isotopic signature ($\delta^{18}O_{sw}^{mod}$) of each micro-slice $\delta^{18}O_{cell}$, using local climate records and species-specific physiological variables, and then compared these values with the $\delta^{18}O$ of local water sources sampled from surface, vadose zone and shallow phreatic zone waters. A synthetic, monthly precipitation isotopic record was also generated to improve our interpretation. We discuss the sub-annual variations in $\delta^{18}O_{sw}^{mod}$ uptake for each species and relate these differences to rooting characteristics, temporal variability in hydrology (discharge and precipitation) and fluvial geomorphology to document how tree water use is controlled by seasonal floodplain water-partitioning.

STUDY AREA

This research is focused in the middle, lowland part of the Rhône River floodplain. The Rhône is a major European river, flowing 512 km from Geneva (French border) to the Mediterranean Sea with a mean annual discharge of 1700 $m^3 s^{-1}$ (Bravard, 2010). The Rhône's flow regime is dominated by snowmelt from its eastern Alpine tributaries, but is also affected by rainfall-generated winter and spring floods. Located 150 km downstream of the Rhône-Saône confluence, the Rhône enters the Tricastin plain, an alluvial geomorphic unit ~25 km in length and ~5 km wide. Because the Rhône was developed for power generation (Bravard, 2010), most of its streamflow bypasses the main stem in this area through the Canal de Donzère-Mondragon, so the riparian forests along the so-called Old Rhône, farther to the west, are subjected to a smaller streamflow water source. The Old Rhône flows along the western edge of the plain at the base of the Cévennes Mountains, part of the Massif Central which is drained primarily by the Ardèche River, the major regional tributary. Since the last glacial period the Tricastin Plain has been extensively reworked by the evolution of river courses (Jean-François, 2011) and is geologically characterized by coarse alluvial sediments (gravel and sand) overlain by sandy-silt that varies in depth from ≤50 cm at the streamside to depths of 2–4 m (Graillot *et al.,* 2010). Between Viviers and the Ardèche-confluence, the Rhône receives groundwater discharge along its right bank, fed by the eastern Massif Central (Graillot *et al.,* 2010).

Our study is focused within a riparian forest site along the right bank of the Old Rhône, situated in the north-western sector of the Tricastin plain, (44.415°N, 4.663°E, 56 m.a.s.l.), part of the commune of Donzère-Mondragon (Figure 2). This site is included within the area of a large restoration programme to ameliorate the impacts of development along the Rhône, L'Observatoire Hommes/Milieux de la Vallée du Rhône (OHM VR) under the auspices of the French National Centre for Scientific Research (CNRS). The forest site covers 0.33 km^2 of the Rhône floodplain, 5 km downstream of a retainer dam which was completed in 1952 to support power generation (Figure 2). The forest stand is a broadleaf community typical of the regional Mediterranean climate, dominated by *F. excelsior* and *P. nigra*. The mean (±SD) growing season (May, June, July and August, MJJA)

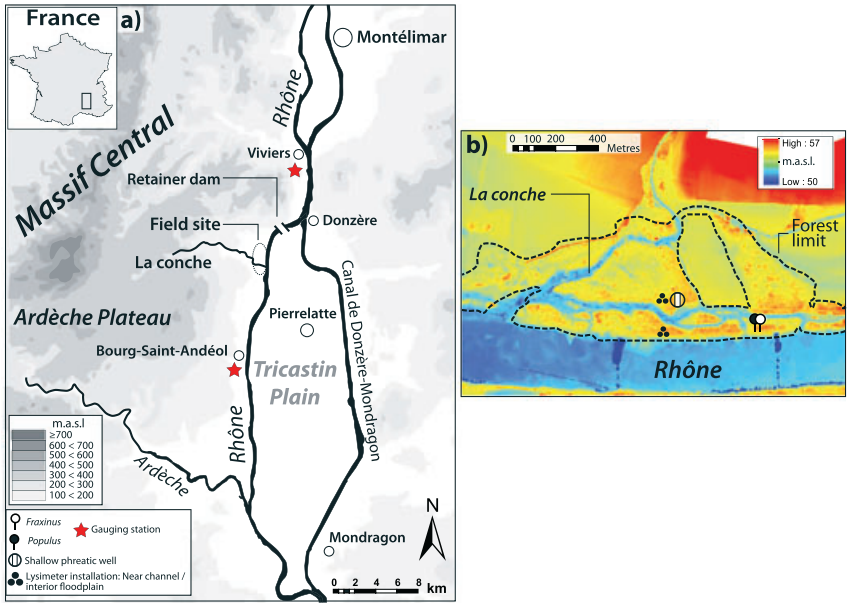

Figure 2. Location of study site (a) within the Tricastin Plain, southern France and (b) LiDAR and equipment locations within the forest site. Topography sourced from 'topographic-map.com' (2015).

temperature is 21.3 ± 3.8 °C, and the mean total precipitation is 200 ± 65 mm respectively, whilst the total annual precipitation is 700 ± 99 mm over the 1999–2010 period. Mean annual discharge (Q) for the site is 234 $m^3 s^{-1}$. The region is characterized by a Mediterranean climate with hot, dry summers and cold, wet winters with rainstorms originating both from the Atlantic Ocean and the Mediterranean Sea (Celle-Jeanton *et al.,* 2001).

METHODOLOGY

Hydro-climate

Climate data (temperature, relative humidity, precipitation, pressure) were downloaded from NOAA's *Global Summary of the Day* (NOAA, 2016) database for the nearby station of Montélimar (44.554868° N, 4.749487° E). Q data were obtained online from the French water agency (www.hydro.eaufrance.fr) for the gauging stations at Viviers (VIV) and Bourg-Saint-Andéol (BSA), upstream and downstream of the retainer dam, respectively. In order to characterize the local Q at our sampling location, linear regression between Q data from Viviers and Bourg-Saint-Andéol was used to extend the shorter BSA Q series (1999–2004) to the present. We quantified growing season and water year (1 September–31 August) totals of P and Q to assess the amount water delivered to the floodplain. Additionally, we computed variables to correspond to a hydrological year—September–August, so we could characterize water available to trees before and during the growing season. In order to assess anomalous climatic years that might be expected to impact water availability to riparian trees from either the vadose or phreatic zone, we classified significant periods of high precipitation and high discharge (P_{high} and Q_{high}) and low precipitation and low discharge (P_{low} and Q_{low}) where seasonal values were $\geq \pm 1\sigma$ of the series mean. We similarly categorized mean growing season temperatures as warm (T_{high}) and cool (T_{low}) and all climatic variables were subdivided into growing season (GS) versus non-growing season (NGS) (Figure 3a, b and c).

Field sampling

Tree-cores. We cored co-located (<5 m apart), mature (>10 m height) and healthy streamside trees of *F. excelsior* and *P. nigra* (DBH of 37 cm and 70 cm respectively) for isotopic analyses using a 5-mm increment borer at breast height. All core samples were obtained in May 2013 and analysed at the University of St Andrews Tree Ring Laboratory, where ring-widths were measured using the Measure JTX tree-ring measuring programme. Raw ring-width measurements were normalized by fitting a 30-year spline to remove ontogenetic trends in ring-width to obtain a growth series for each tree.

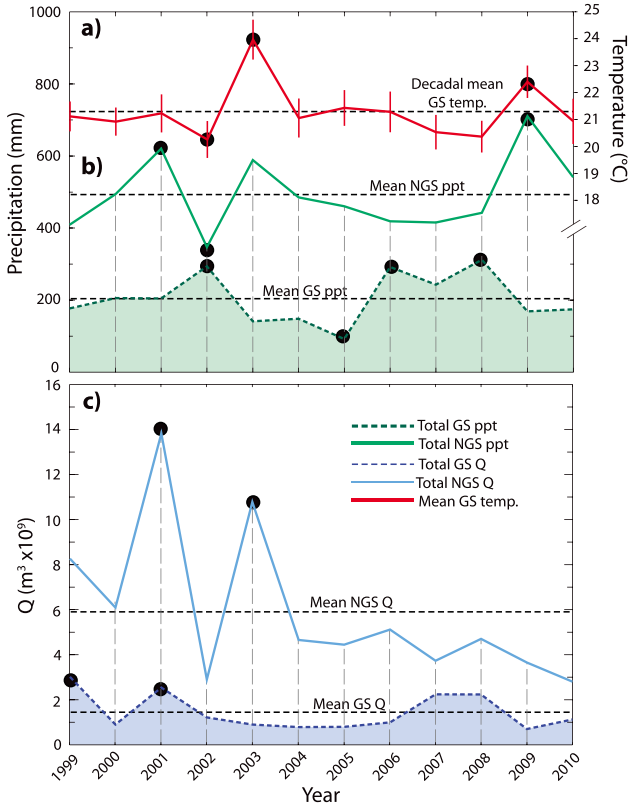

Figure 3. Local environmental variables: (a) mean growing season temperatures; (b) total growing and non-growing season precipitation and (c) total growing and non-growing season discharge. Black dashed lines indicate the series mean and black circles highlight seasons where the respective variable is greater or less than 1 standard deviation of the mean. Temperature error bars are 2 standard errors.

Water source identification. The largely Alpine origin of the Rhône River provides a depleted $\delta^{18}O$ water signature likely to be distinguishable from that of the isotopically enriched, regional water of the Ardèche River (approximately −10‰ and −7‰, respectively [Graillot *et al.,* 2010]). We collected Rhône and Ardèche waters, along with the local floodplain stream 'La Conche', during the growing seasons of 2013–2014 (and then again in Feb 2014). The installation of a shallow (~5 m) well allowed shallow phreatic water samples to be collected during the summer of 2014. We assumed that these contemporary samples would be representative of each isotopic endmember over the 1999–2010 period because $\delta^{18}O$ in Q and groundwater for this basin have low inter-annual variation compared with precipitation (Singer *et al.,* 2014). Sampling of vadose zone moisture was achieved by suction cup lysimeters (1900 L, *Soil Moisture Equipment*) installed at near-channel (<15 m from bank) and interior floodplain (~60 m from bank) positions at depths of 30, 80 and 130 cm. Water samples were extracted under a vacuum of −60 kPa when moisture conditions were sufficiently high. All water samples were stored with no head space in

air-tight 15-ml vials and kept refrigerated prior to analysis at the University of St Andrews isotope laboratory facility.

Precipitation, the major source for vadose zone moisture, varies isotopically on a seasonal basis, reflecting the changes in evaporation/condensation temperatures (Dansgaard, 1964). Furthermore, air-mass origin (Mediterranean v. Atlantic) and mixing can induce seasonal variability in the $\delta^{18}O$ of precipitation, which has been well documented for the south of France (Celle-Jeanton *et al.,* 2001; Delattre *et al.,* 2015). In order to characterize the time-varying isotopic signature of precipitation, we utilized the Global Network of Isotopes in Precipitation (GNIP) (IAEA/WMO, 2015) dataset from the International Atomic Energy Agency for the station at Avignon in conjunction with 'The Online Isotopes in Precipitation Calculator' (OIPC, Bowen, 2015; Bowen *et al.*, 2005), and developed a regression between the monthly values to provide a conversion factor for the Avignon GNIP data. This method incorporates the measured variability in precipitation $\delta^{18}O$, but expresses it for our field site. Where GNIP records were incomplete, we estimated the precipitation $\delta^{18}O_{ppt}$ value from the mean monthly regression of GNIP to OIPC. This allowed for the creation of a synthetic $\delta^{18}O$ time-series that reflects the natural dynamism of seasonal precipitation with the best available local information. We extended this further by computing a mean weighted $\delta^{18}O_{ppt}$ signature for each growing season (MJJA) and non-growing season (September–April, SONDJFMA) to account for the volumetric differences in monthly precipitation delivered to the vadose zone. We also collected rainfall from individual rainstorms during field campaigns on 29th May 2013 and 26th Feb 2014.

Sample preparation and oxygen isotope analyses

We extracted the cellulose within micro-slices from tree rings of two co-located streamside trees (one *F. excelsior* and one *P. nigra*). The small sample size of studied trees was purposeful in order to illustrate and validate our new methodology, rather than to characterize ecohydrology over the entire riparian site, given cost constraints on isotopic analysis. Individual rings for both species, corresponding to the years 2000–2010 (plus latewood from 1999), were visually inspected under a microscope to locate ring boundaries and the position of the earlywood-latewood transition. Micro-slicing was conducted using a sledge microtome with a target mass of 1.5 mg for extraction of α-cellulose for $\delta^{18}O$, which is considered to be the most useful component of wood for this analysis because of its inability to isotopically exchange with other compounds (Wright, 2008; Brookman and Whittaker, 2012). The extraction procedure followed the modified Brendel (mBrendel) method (Gaudinski *et al.,* 2005), adapted for small sample sizes (Evans and Schrag, 2004). Cellulose samples were pyrolized at 1350 °C using a continuous flow Thermo Finnigan High Temperature Conversion/Elemental Analyser (TCEA) connected to a Finnigan Delta plus XP gas source isotopic ratio mass spectrometer (IRMS). Water samples were equilibrated with CO_2 prior to $\delta^{18}O$ analysis via a Thermo Finnigan Gasbench II connected to the IRMS. Oxygen isotope ratios are reported as:

$$\delta^{18}O_{Sample} = \left(\frac{\left({}^{18}O/{}^{16}O \right)_{Sample}}{\left({}^{18}O/{}^{16}O \right)_{VSMOW}} - 1 \right) 1000$$

Our results are expressed in per mil (‰) deviation from Vienna Standard Mean Ocean Water (VSMOW $\delta^{18}O = 2.0052 \times 10^{-3}$‰). Cellulose samples were compared against an IAEA reference standard (IAEA-601 Benzoic acid: +23.3 ± 0.3‰ VSMOW) and an internal lab reference material (Cellulose: +31.05‰ VSMOW).

Modelling seasonal source-water use

The isotopic ratio of cellulosic oxygen is determined by the complex mechanisms occurring during transpiration and biosynthesis. No isotopic fractionation occurs during the uptake of source water by roots (Dawson and Ehleringer, 1991), but water movement through the plant is driven by transpiration of water through leaf stomata, which enriches the leaf water in the heavy isotope (Craig and Gordon, 1965; Dongmann *et al.,* 1974; Flanagan and Ehleringer, 1991). The level of enrichment is a function of the interactions between air temperature, atmospheric pressure, humidity and the $^{18}O/^{16}O$ content of ambient water vapour ($\delta^{18}O_{wv}$), modified by rates of stomatal conductance and transpiration, in addition to a Péclet effect—the balance between isotopic advection and diffusion at the leaf boundary (Barbour *et al.,* 2004). The leaf water isotopic signature is imparted into sucrose via carbonyl oxygen exchange but with a 27 ± 4‰ enrichment factor (Yakir and DeNiro, 1990). This isotopic signature remains unaltered until the sucrose molecule is cleaved during cellulose synthesis, enabling a portion of the oxygen atoms to exchange with xylem source water (Hill *et al.,* 1995). The fraction of oxygen atoms exchanged has been reported as 0.42 for a number of riparian trees and acts to dampen the leaf-level enrichment signal (Roden *et al.,* 2000).

To determine the $\delta^{18}O_{sw}$ used by the tree to form each micro-sliced cellulose sample, we used the mechanistic model of Barbour *et al.* (2004) coded in Matlab (version R2013a) to run inversely in order to predict $\delta^{18}O_{sw}$ from known $\delta^{18}O_{cell}$, climate variables and species-specific transpiration/conductance values. An important prerequisite here is that climate input variables must correspond to the timing of cellulose formation. Recent research by Cuny *et al.* (2015) has shown that in some coniferous species

biomass deposition lags behind stem girth growth by approximately one month. If this lag were well quantified for relevant tree species, it could be used to lag shift the climatic series. However, given the lack of such information for our deciduous tree species we must assume a linear rate of biomass production. On this basis we assigned a date to each micro-slice based on its relative position in the growth increment (*à la* Verheyden *et al.,* 2004; Berkelhammer and Stott, 2009). Earlywood and latewood samples were attributed to the months of May-July and August, respectively. We accounted for the climatic conditions contributing to the $\delta^{18}O_{cell}$ of each micro-slice by using the mean temperature, relative humidity and pressure for the days leading up to the assigned sample date and starting from the date used for the previous micro-slice (supp. material) (*Global Summary of the Day*, Montélimar). We utilized mean stomatal conductance and transpiration values presented in Lemoine *et al.* (2001) for *F. excelsior* ($0.2\,mol\,m^{-2}\,s^{-1}$/$3.9\,mmol\,m^{-2}\,s^{-1}$) and Lambs *et al.* (2006) for *P. nigra* ($0.278\,mol\,m^{-2}\,s^{-1}$/$4.73\,mmol\,m^{-2}\,s^{-1}$). An effective path length of 4.3 cm was used for the Péclet effect parameter of the model, which has been previously employed for these species within another Rhône site (Singer *et al.,* 2014).

To characterize the $\delta^{18}O_{wv}$ throughout the growing season, we assumed that precipitation and atmospheric water vapour were in isotopic equilibrium and applied an offset of $-10‰$ from the synthetic precipitation series for growing season months to obtain a time-varying $\delta^{18}O_{wv}$ dataset that accounts for the dynamic effects of air mass origin and mixing for the region (Bowen and Wilkinson, 2002; Celle-Jeanton *et al.,* 2001; Delattre *et al.,* 2015).

Our date assignment for each micro-slice ensured that we accounted for the seasonal progression and variability in climate variables. We qualified this assumption, along with the premise of linear deposition of biomass, with an estimate of uncertainty based on 1000 Monte-Carlo simulations selecting from the range of growing season RH and T for each micro-slice.

All statistical analyses were conducted in the statistical software package Minitab (version 17) and are reported relative to the 95% significance level. For correlation analyses we utilized Spearman's rank (r_s), the T-test (T) for comparing the means of two sample sets whilst ANOVA (F) was used for comparing the means of more than two datasets followed by post-hoc tests to determine where differences occurred in the event of a statistically significant ANOVA result.

RESULTS AND INTERPRETATIONS

The following section details the main findings of the study, separated into subsections which include a brief interpretation.

Discharge, precipitation and temperature

Over the time series, P_{high} occurred in the NGS2001 and NGS2009 and GS2002, GS2006 and GS2008, whereas P_{low} occurred for the NGS2002 and the GS2005 (Figure 3a, b and c). Q_{high} occurred in both seasons for 2001, whereas Q_{high} in 1999 and 2003 only occurred in one season—the GS and NGS, respectively. The GS2009 and NGS2010 produced the lowest seasonal discharge totals in the series. GS T_{high} occurred in 2003 and 2009 and T_{low} in 2002, indicating that 2003/2009 have the potential for relatively high evaporation of vadose zone water. Comparing the contribution of streamflow in the GS to water-year Q totals provides information on the potential hyporheic contribution to the floodplain water table contemporaneous with growth. The largest contribution was in 2007 (38%) and the lowest in 2003 (8%), suggesting that the former would produce an elevated GS water table compared to the latter. Similarly, the partitioning of seasonal precipitation affects water availability in the vadose zone and its isotopic signature. The largest GS precipitation contribution (46%) occurred in 2002 and the smallest (17%) in 2005. No significant correlation exists between the seasonal totals of precipitation and discharge (NGS, $r_s = 0.175$, $p = 0.587$; GS, $r_s = 0.567$, $p = 0.054$), suggesting that there is a hydrological disconnect between these two sources of water in this part of the Rhône basin.

Precipitation and streamflow appear to be climatically disconnected, which suggests that they each have an internal variability driven by different parts of the hydrological cycle that may directly impact the water availability at particular rooting depths.

Potential source water $\delta^{18}O$ signatures. The GS Rhône water $\delta^{18}O$ was significantly more depleted than other surface water sources in the region (e.g. Ardèche river and the local surface waters), indicating a snowmelt origin (Graillot *et al.,* 2010; Singer *et al.,* 2014) (Figure 4). In contrast, the Ardèche River, local tributaries (Central Massif origin), and shallow phreatic waters are relatively enriched and isotopically similar to one another, suggesting a common, regional recharge zone which is supplied by NGS precipitation (NGS $\delta^{18}O_{ppt}$) (Table I). We note that the $\delta^{18}O$ in samples of NGS Rhône water were isotopically enriched compared to the GS Rhône water, which may be reflective of a predominantly precipitation signal in these months compared with the snowmelt signature of the growing season, but the small number of water samples ($n = 2$) limits a detailed interpretation.

The time series of calculated mean monthly precipitation $\delta^{18}O$ displayed the expected seasonality of enriched summer and depleted winter precipitation. We assessed the isotopic signature of seasonal precipitation contributions (NGS/GS $\delta^{18}O_{ppt}$) by weighting the mean values of $\delta^{18}O$ by

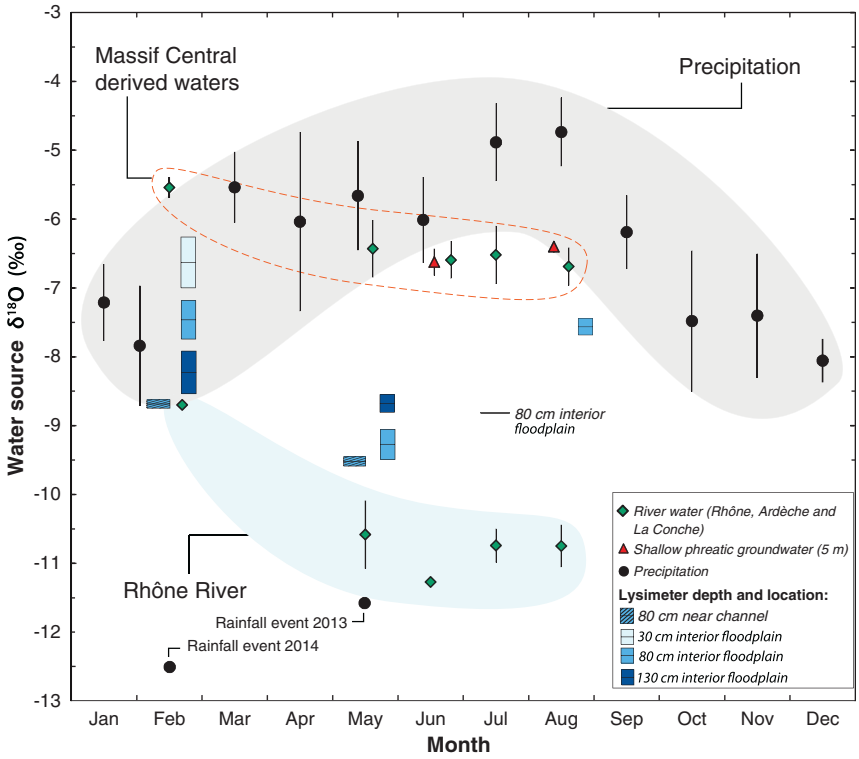

Figure 4. Monthly $\delta^{18}O$ characteristics of potential endmember water sources for Donzere Mondragon. Precipitation values represent the arithmetic (non-weighted) mean of monthly $\delta^{18}O$ precipitation for the study period. Calculations were based on Global Network of Isotopes in Precipitation (GNIP), Bowen (2015) The Online Isotopes in Precipitation Calculator, version 2.2. (www.waterisotopes.org) and Bowen *et al.*, 2005. Surface water samples were collected during each respective month for 2013 and 2014 (lysimeter and phreatic water data were collected in 2014). No data available for near channel lysimeters at 30 cm and 130 cm depth.

Table I. Potential endmember water-sources, sample sizes and mean values of $\delta^{18}O$. Values followed by superscript letters are statistically similar ($F_{7,53} = 85.48$, $p < 0.001$). A margin of ±2SE around the means is indicated in parentheses.

Water source	*n*	Mean $\delta^{18}O$ value (‰)
Rhône water growing season	10	−10.8 (±0.2) [d]
Rhône water non-growing season	2	−8.7 (±0.0) [e]
Surface water growing season	10	−6.5 (±0.2) [b c]
Surface water non-growing season	4	−5.6 (±0.1) [a b]
Ardèche water growing season	4	−6.7 (±0.2) [b c]
Shallow phreatic growing season	9	−6.9 (±0.7) [c]
Precipitation growing season (weighted)	11	−5.5 (±0.4) [a]
Precipitation non-growing season (weighted)	11	−7.1 (±0.4) [c]

monthly precipitation totals (Figure 5a and 5b). The seasonal difference in $\delta^{18}O_{ppt}$ was 1.6‰ (higher in the GS), but with seasonal similarities in 2002 and 2007 (Figure 5c). We also observed large, isotopically depleted precipitation totals for the NGS2009, which produced a $\delta^{18}O_{ppt}$ of −8.8‰, the most depleted for the entire time period. Because air masses within the Rhône valley have different oceanic origins and associated values of vapour $\delta^{18}O$ (north Atlantic-depleted, Mediterranean-enriched) (Celle-Jeanton *et al.,* 2001), individual precipitation events can differ substantially from monthly means and therefore give rise to, for example, anomalously depleted $\delta^{18}O$ values for rainfalls recorded in May 2013 (−11.6‰) and February 2014 (−12.5‰), which suggest air masses of north Atlantic origin.

The isotopic analyses of lysimeter waters provide more direct evidence of the isotopic signature of water available to vadose zone tree roots. These data indicate a well-mixed zone existed at the interior floodplain site (surface elevation of 54.6 m.a.s.l.) at 130 cm depth, which remained isotopically stable from February to May (Figure 4). The lack of available moisture for extraction at 130 cm depth at the near channel site is likely because of its higher surface elevation (55.4 m.a.s.l.), its proximity to the riverbank and coarser material properties, as it sits on a natural levee.

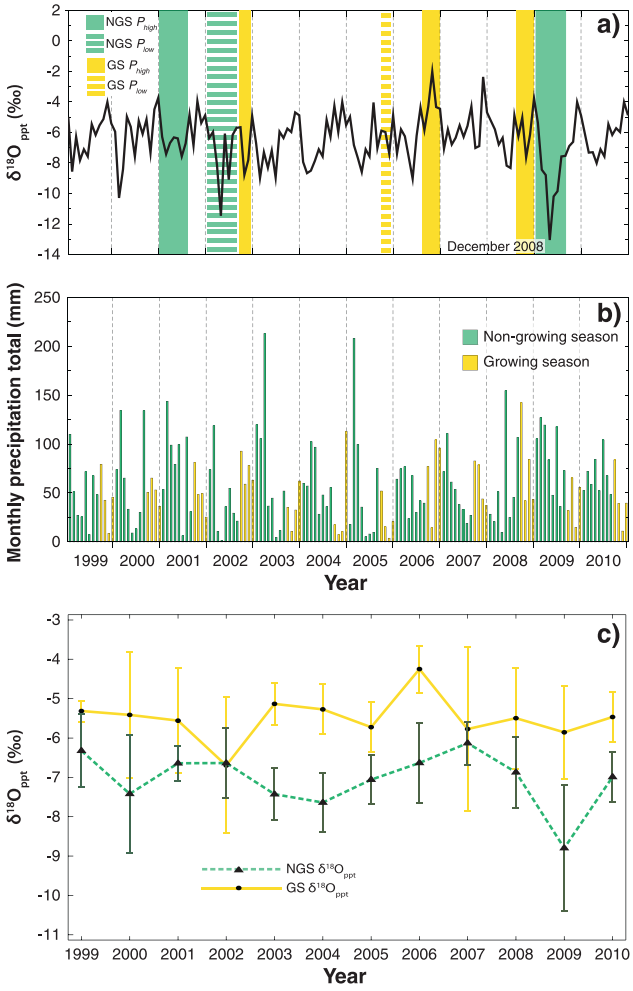

Figure 5. Precipitation data: (a) synthetic δ18O of monthly precipitation with hydrologic classification; (b) monthly precipitation totals for water years 1999–2010 and (c) the weighted seasonal isotopic signatures of precipitation (δ18Oppt), bars are 2 standard errors. Synthetic δ18O values based on Avignon station data from Global Network of Isotopes in Precipitation (GNIP) and Bowen (2015) The Online Isotopes in Precipitation Calculator, version 2.2. (www.waterisotopes.org) and Bowen *et al.*, 2005.

In the interior floodplain at 30 cm depth, soil water could only be extracted in February 2014, and it had a $\delta^{18}O$ value comparable to the precipitation February mean $\delta^{18}O$, indicating that the vadose zone is largely composed of moisture derived from precipitation during the wetter NGS, whilst GS rainfall does not contribute significantly to the overall soil moisture $\delta^{18}O$ signature in most years. In fact, it appears that water from GS rainstorms is rapidly evaporated or taken up through transpiration by tree roots from upper soil layers (e.g., lack of water in soil at 30 cm for both near-channel and interior floodplain locations Figure 4). In contrast, the NGS precipitation appears to infiltrate down to an isotopically well-mixed zone at 130 cm (interior floodplain). The seasonal variation in soil moisture $\delta^{18}O$ at 80 cm depth for both floodplain positions (soil water is enriched in winter and depleted in summer), contrasts with the seasonal pattern of precipitation $\delta^{18}O$ (Figure 4), suggesting a significant lag time for precipitation to infiltrate into the top meter of the vadose zone. Thus, the isotopic value at 130 cm would be expected to shift downward in June/July once the wetting front from NGS rainfall reached this depth.

The strong isotopic differences between NGS and GS precipitation allow for the seasonal discrimination of moisture inputs within the vadose zone. Hyporheic discharge provides highly depleted source water to the phreatic zone which contrasts to the enriched regional groundwater in this site. These differences demonstrate good potential to identify the source of water delivered to contrasting rooting zones of *Fraxinus* and *Populus*.

Cellulosic oxygen ($\delta^{18}O_{cell}$). *F. excelsior* had a higher sub-annual variability in $\delta^{18}O_{cell}$ over the decade compared to *P. nigra* (SD = 1.2‰ and 0.7‰ respectively), whilst the series means revealed that *Fraxinus* likely used water that was substantially more enriched in ^{18}O (30.7‰) than *Populus* (28.7‰) (Figure 6a), assuming these large differences are not because of leaf water fractionation. The $\delta^{18}O_{cell}$ of earlywood and latewood over all years was significantly different for *Fraxinus* but not for *Populus* ($F_{3,244} = 154.36$, $p < 0.001$), and the two tree species exhibited no covariance in $\delta^{18}O_{cell}$ ($r_s = -0.136$, $p = 0.689$) even though their annual means were statistically indistinguishable in many water years: 2002, 2005, 2007, 2009 and 2010 ($F_{21,213} = 33.49$, $p < 0.001$). We also observed an apparent shift towards inter-species $\delta^{18}O_{cell}$ coherence following the year 2006, concomitant with a reduction in sub-annual $\delta^{18}O_{cell}$ variability for both trees (Figure 6a). Visual comparison of micro-slice $\delta^{18}O_{cell}$ against mass-weighted $\delta^{18}O_{cell}$ of whole rings demonstrated that considerable isotopic information is masked through whole-ring analyses, for example the difference between the weighted mean $\delta^{18}O_{cell}$ of *Fraxinus* in 2001 and 2002 is only 0.1‰, yet these years are markedly different in their seasonal pattern of $\delta^{18}O_{cell}$. This high-resolution information becomes particularly important where individual sub-annual $\delta^{18}O_{cell}$ values exceed the weighted mean of the other species. For example water years 2000, 2003, 2005, 2009 and 2010 reveal individual *Fraxinus* $\delta^{18}O_{cell}$ values that are more depleted than the weighted mean of *Populus* $\delta^{18}O_{cell}$. For *Fraxinus*, earlywood contributed to 45% of the ring mass, whilst this was substantially greater for *Populus* (80%), suggesting different seasonal strategies of water use and growth.

The strong variability in sub-annual $\delta^{18}O_{cell}$ for both species suggests that important seasonal information relating to tree-level and climatic processes is retained within each ring. The $\delta^{18}O_{cell}$ results indicate a period when the isotopic values of both species synchronize, which may suggest a change in controlling hydrology.

Modelled source-water ($\delta^{18}O_{sw}^{mod}$). Despite clear differences in $\delta^{18}O_{cell}$ between trees, these values cannot be easily

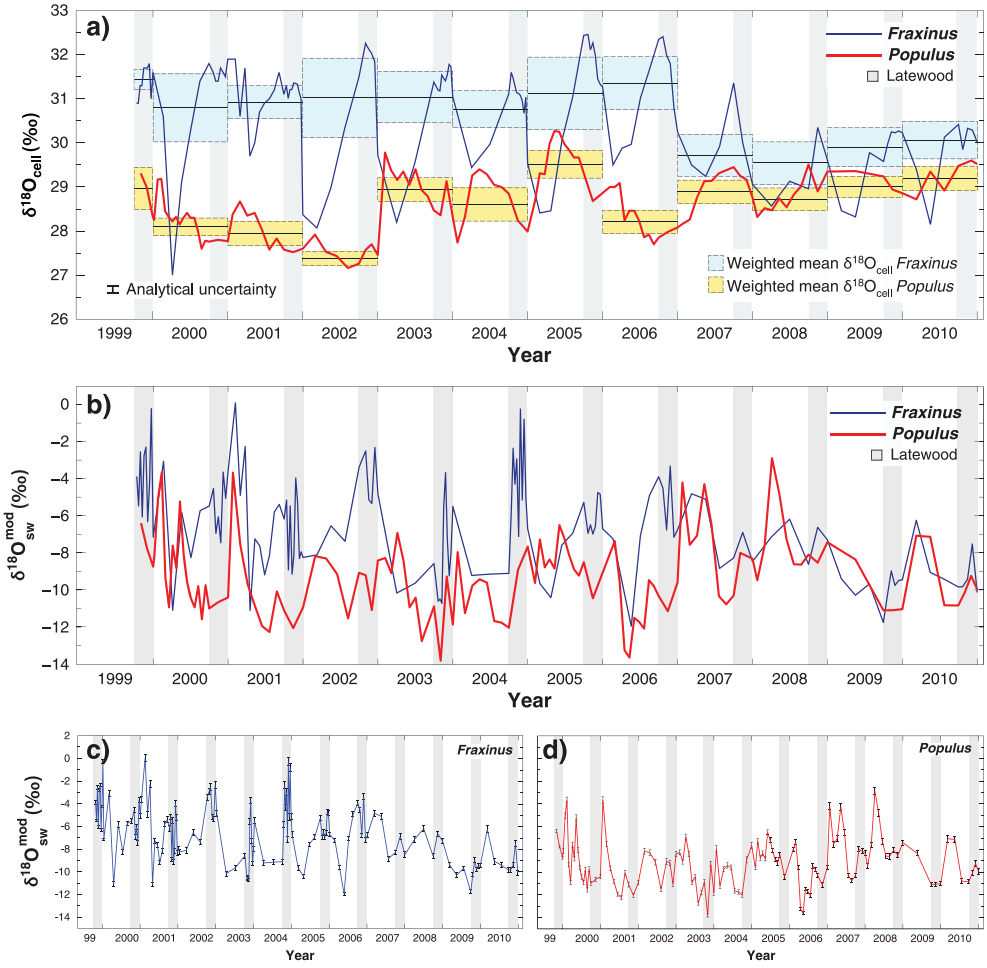

Figure 6. Results of sub-annual micro-slicing of *F. excelsior* and *P. nigra*: (a) δ18Ocell for individual microslices (1999 latewood only) superimposed on mass weighted means of δ18Ocell for each ring (±2 S.E.), (b) modelled source-water use (δ18Osw) of *F. excelsior* and *P. nigra* and modelled δ18Osw with Monte-Carlo simulated variability indicated by error bars for (c) *F. excelsior* and (b) *P. nigra*.

interpreted in terms of the $\delta^{18}O_{sw}$, owing to the fractionations at the leaf level and during cellulose synthesis that may mask source water differences. The inverse modelling of $\delta^{18}O_{sw}$ ($\delta^{18}O^{mod}_{sw}$) (Figure 6b, c and d) provides a clearer picture of seasonal water usage by trees. These model results showed that overall *Fraxinus* $\delta^{18}O^{mod}_{sw}$ was more enriched (−6.7‰) compared to *Populus* $\delta^{18}O^{mod}_{sw}$ (−9.2‰) ($T_{246} = 8.42$, $p < 0.001$) (Figure 6b), which suggests a strong difference in water source delivered to the rooting zone of each species. *Fraxinus* displayed greater variability in water source usage than *Populus* (Figure 6b); however, the difference is not significant ($T_{22} = 0.81$, $p = 0.428$). Generally, the sub-annual progression of $\delta^{18}O^{mod}_{sw}$ in *Fraxinus* followed a pattern of depleted water in the earlywood followed by progressive enrichment into the subsequent latewood fraction. Across the decadal series, the latewood component of *F. excelsior* is 1.1‰ more enriched than its earlywood ($T_{110} = -2.483$, $p = 0.017$). For *P. nigra* the sub-annual pattern of $\delta^{18}O^{mod}_{sw}$ was similar to that of *Fraxinus*, although the earlywood depletion proceeded intermittently rather than monotonically and at a reduced rate. Despite the mean latewood $\delta^{18}O^{mod}_{sw}$ being 0.8‰ more depleted than the earlywood ($T_{54} = 2.05$, $p = 0.046$) for *Populus*, the individual sub-annual latewood values showed a pattern towards a more enriched $\delta^{18}O^{mod}_{sw}$ with procession of latewood growth.

Similar to the $\delta^{18}O_{cell}$ results, the $\delta^{18}O^{mod}_{sw}$ values for both trees show a convergence for the 2007–2010 period, whereby the previously dissimilar series mean $\delta^{18}O^{mod}_{sw}$ values for *Fraxinus* and *Populus* (2000–2006) become coherent ($F_{3,231} = 32.03$, $p < 0.001$). This shift towards a common $\delta^{18}O^{mod}_{sw}$ is accompanied by reduced sub-annual variability for *Fraxinus* $\delta^{18}O^{mod}_{sw}$ (−0.9‰) and an increase in variability for *Populus* $\delta^{18}O^{mod}_{sw}$ (+0.1‰) compared to the preceding years. Comparison of pairs of mean annual $\delta^{18}O^{mod}_{sw}$ between trees for each year (Figure 7a) highlights the transition, but it also identifies 2003 (NGS Q_{high}) and 2005 (GS P_{low}) as years when both species apparently shared a common water source ($F_{21,\ 213} = 7.57$, $p < 0.001$). However, the onset of the shift in 2007 cannot be attributed to a discharge or precipitation anomaly.

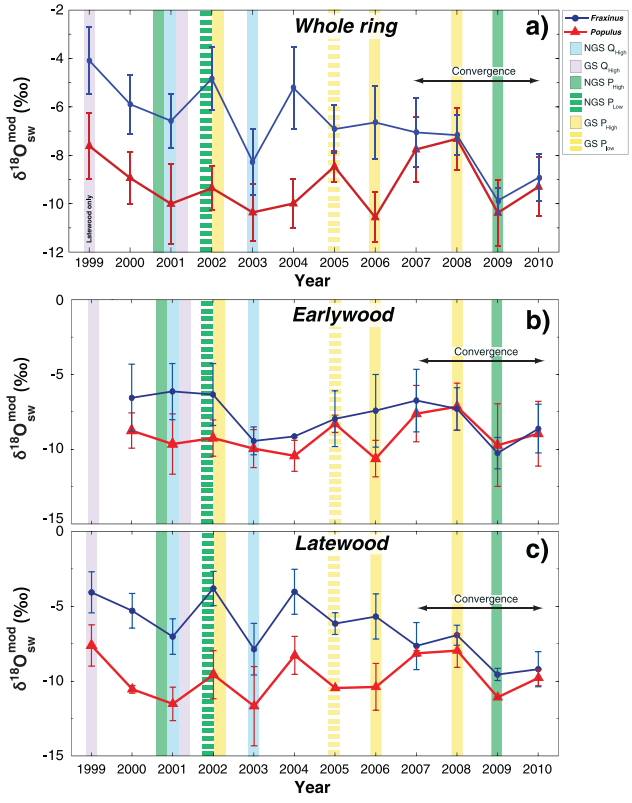

Figure 7. Time series of: (a) the mean annual modelled $\delta^{18}O_{sw}$ of *Fraxinus* and *Populus* (1999 latewood only). The years 2003, 2005, 2007, 2008, 2009 and 2010 are where the concurrent means of both species are similar ($F_{21,\ 213} = 7.57$, $p < 0.001$); and comparisons of the mean $\delta^{18}O_{sw}$ for the (b) earlywood and (c) latewood fractions for *Fraxinus* and *Populus*. Error bars represent 2 standard errors.

The convergence period of $\delta^{18}O^{mod}_{sw}$ is also evident at the sub-annual level (Figure 7b and c). The earlywood and latewood $\delta^{18}O^{mod}_{sw}$ values for both species were tightly coupled ($F_{7,\ 240} = 18.98$, $p < 0.001$), which contrasts with 1999–2006 in which only the two species' latewood fractions co-varied, although they remained isotopically distinct.

Overall, *Fraxinus* demonstrated a more pronounced trend in its seasonal $\delta^{18}O^{mod}_{sw}$ compared to *Populus*, indicating source water usage differences between species. We identified a period of convergence in seasonal $\delta^{18}O^{mod}_{sw}$, which suggests that one or both species may have switched from its preferred source of water for the duration of the 2007–2010 growing seasons to a common water source.

Species source-water ($\delta^{18}O^{mod}_{sw}$) and seasonal precipitation ($\delta^{18}O_{ppt}$). The $\delta^{18}O^{mod}_{sw}$ of *F. excelsior* tracked the seasonal $\delta^{18}O_{ppt}$ signatures, which is consistent with rooting depth and the uptake of vadose zone moisture (Singer *et al.*, 2013, Figure 1). The lack of statistical difference between *Fraxinus* earlywood $\delta^{18}O^{mod}_{sw}$ and NGS precipitation $\delta^{18}O$ ($T_{42} = 6.34$, $p = 0.823$) during the 2000–2006 period suggests a reliance on this seasonal precipitation for earlywood growth, where low evaporative conditions preserve the NGS $\delta^{18}O_{ppt}$ signal within the soil profile. Water used for latewood growth is likely sourced from enriched GS precipitation (no statistical difference in sample means: $T_{37} = 0.26$, $p = 0.794$) (Figure 8a), as the $\delta^{18}O$ of the vadose moisture pool evolves from the top of the soil column downward in response to GS rainfall.

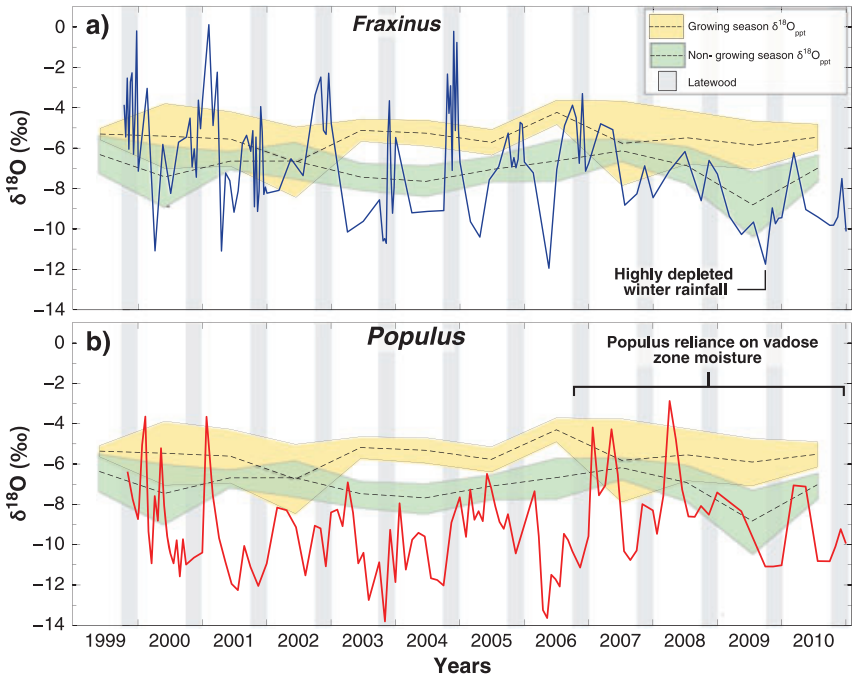

Figure 8. Time series of growing and non-growing season $\delta^{18}O_{ppt}$ in relation to: (a) *F. excelsior* and (b) *P. nigra* modelled $\delta^{18}O_{sw}$. Dashed lines are the mean $\delta^{18}O_{ppt}$ values, and coloured spread is 2 standard errors for each respective seasonal series.

Infiltrated precipitation water is further enriched by evaporative losses from the vadose zone under elevated growing season temperatures (Gazis and Feng, 2004). Such processes are recorded as enriched $\delta^{18}O_{sw}^{mod}$ values within the latewood component of *Fraxinus* rings (Figure 8a), specifically where $\delta^{18}O_{sw}^{mod}$ exceeds GS $\delta^{18}O_{ppt}$ (e.g. latewood 1999, 2002 and 2004). We attribute intra-annual deviations in latewood $\delta^{18}O_{sw}^{mod}$ enrichment (e.g. 2004, Figure 8a) to the uptake of depleted precipitation from isolated storms (e.g. May 2013), which infiltrate the soil profile during the GS. In instances where latewood $\delta^{18}O_{sw}^{mod}$ values become more depleted than GS $\delta^{18}O_{ppt}$ (e.g. 2001, 2003, 2004, 2005, Figure 8a), these may reflect transient access to non-mobile soil water during periods of high transpiration. This pore bound (low matric potential) water has been shown in another Mediterranean environment to retain the isotopic signal of NGS rainfall events (Brooks *et al.,* 2010). Our inability to extract moisture at 30 and 80 cm suggests that during drier conditions *Fraxinus* may draw on these tightly bound moisture pools. During the 2007–2010 period, the lack of statistical differences suggest that *Fraxinus* relied almost entirely on NGS $\delta^{18}O_{ppt}$ for the production of earlywood ($T_8 = 1.43$, $p = 0.190$) and latewood ($T_7 = 1.37$ $p = 0.214$). However, water years 2007 and 2008 provide evidence for growing season precipitation uptake which may be the result of the larger data spread in GS rainfall $\delta^{18}O$ values (Figure 8a). The depleted and NGS P_{high} in 2009 was clearly recorded by *Fraxinus*. We suggest that the preservation of this water-source signature is a function of highly depleted, non-growing season P_{high} in 2009 in addition to a below average growing season precipitation total and elevated temperature (T_{high}).

During the pre-2007 period, the $\delta^{18}O_{sw}^{mod}$ of *P. nigra* reflected a depleted water source that was different to vadose (precipitation) moisture used by *F. excelsior*, with earlywood and latewood values that were statistically different to NGS $\delta^{18}O_{ppt}$ ($T_{44} = 8.000$; $T_{21} = 6.34$, $p < 0.001$) and GS $\delta^{18}O_{ppt}$ ($T_{18} = 10.78$, $T_{23} = 9.10$; $p < 0.001$). Although *P. nigra* periodically utilized enriched water, similar to that of GS $\delta^{18}O_{ppt}$ (e.g. 2001, 2002 and 2005), these values were not concomitant with vadose zone moisture (precipitation-derived) uptake by *Fraxinus* (Figure 8a and b) (but see early GS 2000). The absence of a statistical difference between the $\delta^{18}O_{sw}^{mod}$ of *Populus* earlywood and NGS $\delta^{18}O_{ppt}$ ($T_8 = 0.91$, $p = 0.389$) suggests that from 2007 onwards there is reliance on vadose zone moisture, supported by a strong similarity between both species for the latewood $\delta^{18}O_{sw}^{mod}$ (Figure 8b). The highly depleted NGS precipitation totals in 2009 were also clearly recorded by both species. These factors suggest that both species rely on the same moisture pool (vadose zone) as the growing season progressed during each year of the convergence period.

There is a strong similarity between ($\delta^{18}O_{ppt}$) and *Populus* $\delta^{18}O_{sw}^{mod}$ which suggests this species and *Fraxinus* are relying on vadose zone water from 2007 to 2010. The sub-annual $\delta^{18}O_{sw}^{mod}$ of *Fraxinus* shows uptake of vadose zone moisture derived from NGS (earlywood) and GS (latewood) precipitation. From 2007 *Fraxinus* appears to rely on only NGS precipitation for growth.

Species source-water ($\delta^{18}O_{sw}^{mod}$) and phreatic water ($\delta^{18}O$). The deep rooting zone of *Populus* allows it to access water from the Rhône River ($\delta^{18}O$: -10.8 ± 0.2‰) and Central Massif-derived groundwater (shallow phreatic $\delta^{18}O$: -6.9 ± 0.7‰). In the period 2000–2006, the isotopic signature of earlywood micro-slices is similar to that of shallow phreatic (Massif Central derived) water, followed by depleted $\delta^{18}O_{sw}^{mod}$ values that are comparable to Rhône water (Figure 9a). These depleted $\delta^{18}O_{sw}^{mod}$ values then become enriched at the end of the earlywood into the latewood component of the annual ring. There are several instances when *Populus* $\delta^{18}O_{sw}^{mod}$ values are more enriched than those of *Fraxinus* (e.g. 2000, 2003, 2005 earlywood; Figure 9a). These factors suggest a poor relationship between *Populus* water usage and precipitation-derived vadose zone water in the pre-convergence period (e.g. GS $\delta^{18}O_{ppt}$; Figure 8b). To explain the sub-annual pattern of *Populus* $\delta^{18}O_{sw}^{mod}$, we suggest a 'bank storage' effect (Alaghmand *et al.,* 2014), in which the river supplies depleted waters (i.e. during spring snowmelt in the early GS) to the alluvial aquifer by hyporheic flow, first mixing with and then dominating over the enriched regional groundwater. The hyporheic water later recedes as the snowmelt hydrograph declines (late GS), allowing the water of the Massif Central to enrich the phreatic zone, which becomes available for latewood (and the following growing season earlywood) growth. The highly depleted values of *Populus* $\delta^{18}O_{sw}^{mod}$ values are linked to periods of higher river discharge (e.g. 2001 and 2003) supplying hyporheic water to the rooting zone, yet there is no overall correlation between mean *Populus* $\delta^{18}O_{sw}^{mod}$ and seasonal discharge totals (NGS: $r_s = 0.227$, $p = 0.502$; GS: $r_s = 0.351$, $p = 0.290$). Furthermore, in 2006 *Populus* displayed sustained and depleted $\delta^{18}O_{sw}^{mod}$ values (minimum value: -13.6 ‰), which suggests that there is complex interplay between river discharge, providing depleted $\delta^{18}O$ waters, and that of the enriched Central Massif groundwater, especially for these streamside trees (Dawson and Ehleringer, 1991).

The cumulative discharge totals reveal a tentative association between: the rate of transition to and from depleted values of *P. nigra* $\delta^{18}O_{sw}^{mod}$ over the course of the growing season; the timing of flood peaks; and NGS discharge and GS discharge (Figure 9a and b). Rapid declines in *Populus* $\delta^{18}O_{sw}^{mod}$ (e.g. 2003) may be the result of greater a NGS to GS discharge ratio (Figure 9b), which provides a large influx of depleted river water to the phreatic zone during early water year flood peaks, but

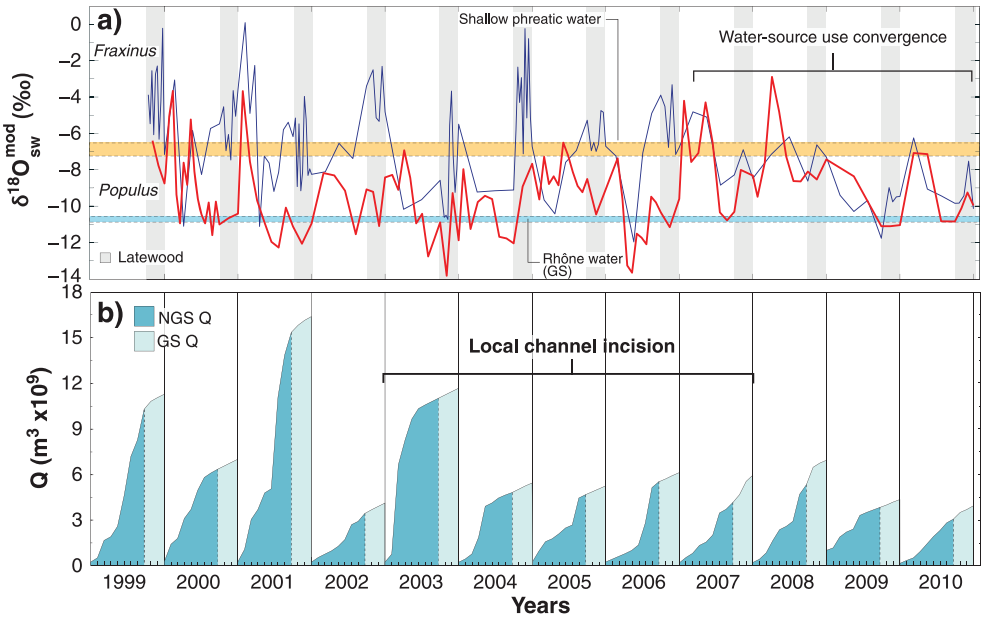

Figure 9. Time series of: (a) Modelled sub-annual tree $\delta^{18}O_{sw}$ values and the mean (±2 SE) Rhone River (growing season) and shallow phreatic water (growing season) $\delta^{18}O$; and (b) time series of cumulative discharge for the Old Rhône River.

which is rapidly returned to enriched Massif Central waters because of relatively low GS discharge.

We would expect *Populus* to rely on vadose moisture (i.e. from 2007) as the result of water table lowering (Singer *et al.,* 2013, 2014), but discharge data on their own (Figure 3c, 9b) do not support this hypothesis.

There was no correlation between annual mean *Fraxinus* $\delta^{18}O_{sw}^{mod}$ (2000–2010) and NGS Q total ($r_s = 0.218$, $p = 0.519$) or GS Q totals ($r_s = 0.137$, $p = 0.689$), which is understandable for this shallowly rooting species. However, during high flow years (e.g. 2000, 2001 and 2003) we note a more sustained depletion (v. transient events) in *Fraxinus* $\delta^{18}O_{sw}^{mod}$ values, which are not in sync with NGS $\delta^{18}O_{ppt}$ values. We attribute such 'events' to peaks in NGS Q which act to raise the water table height into the overlying fine-grained layer (or even overbank), providing periodic access of depleted $\delta^{18}O_{sw}$ to *Fraxinus* roots, aided by capillary action (Sánchez-Pérez *et al.,* 2008) (Figure 9a/b).

Populus apparently uses phreatic water derived from two distinct sources, depleted river water and enriched regional groundwater, which produces a pattern of seasonal variation in $\delta^{18}O_{sw}^{mod}$ values. From 2007–2010 *Populus* apparently relies on vadose moisture suggesting a separation between phreatic water and the rooting zone, perhaps associated with a loss of access to the water table.

DISCUSSION

Previous studies of sub-annual variability in tree-ring oxygen isotopes have identified changes in seasonal water uptake in response to climatic forcing (e.g. Barbour *et al.,* 2002; Sarris *et al.,* 2013), but there is a lack of focus in the literature on relating these changes to the discrete hydrological processes which control the availability of water at the rooting zone. Furthermore, to date, most studies have relied on differences between cellulosic isotope values from tree rings to infer water source variations, without deconvolving the actual signature of source water (Marshall and Monserud, 2006; Singer *et al.,* 2013). There are two notable exceptions we have identified in the literature. Williams *et al.* (2005) obtained the isotopic signature of source water used by archaeological maize by back-calculating using the Roden *et al.* (2000) tree-ring model. Subsequently, Singer *et al.* (2014) used inverse modelling from tree ring $\delta^{18}O_{cell}$ via the Barbour *et al.* (2004) model (an enhancement of the Roden model) to determine annually averaged water sources used by riparian trees at an upstream site along the Rhône. However, this method remains notably underutilized for documenting historical records of tree water-source use, especially on seasonal timescales. In this paper, we expand on previous work by employing inverse bio-mechanistic modelling of $\delta^{18}O_{sw}^{mod}$ used in tree-ring cellulose synthesis and comparing these values to the $\delta^{18}O$ of all relevant *in situ* water sources to improve interpretations of sub-annual isotopic variations. Our aim was to test the utility of this method for reconstructing the seasonal ecohydrological interactions within a floodplain setting in response to climatic forcing of water availability to riparian trees. We highlight and discuss several important outcomes of this research below.

First, consistent with prior research, we found that substantially more isotopic information is obtained through micro-slicing of individual tree-rings compared to whole ring analyses alone (e.g. Roden *et al.,* 2009), and this information provides a window into patterns of seasonal water use by riparian trees obtaining water from different floodplain water sources. Our sub-annual $\delta^{18}O_{cell}$ measurements, for both species, exhibited considerable variation around both the whole-ring weighted mean and its variance (Figure 6a), which we attribute to seasonal variation in their respective water-source use strategies. Indeed, variability in source water $\delta^{18}O$ has been considered to be the main driver in $\delta^{18}O_{cell}$ variability within individual rings (Treydte *et al.,* 2014). Assessment of these seasonal fluctuations in water use is vital for understanding how the hydrological cycle is expressed within water availability to trees. Such detailed information is fundamental to forensic analysis of tree responses to water scarcity, especially in Mediterranean forests (e.g. Bréda *et al.,* 2006) and to forecasting of forests responses to future climate, yet annual measurements of $\delta^{18}O_{cell}$ provide a limited and potentially skewed record of water availability that could engender erroneous interpretations of tree water use. For example, if one considers years as either 'dry' or 'wet' based on annual means of precipitation and discharge, these generalizations belie the fact that hydrological conditions affecting water availability fluctuate throughout the year and some parts of the water year may play a disproportionate role in generating root zone moisture. In such cases, annual tree-ring isotopic signatures may be at odds with the governing hydrological conditions, especially if there is a species' reliance on seasonal water source contributions for a particular stage of growth (e.g. *Fraxinus* earlywood and latewood components).

Second, to our knowledge this is the first study to interpret micro-slice $\delta^{18}O_{cell}$ variations on a historical timescale of decades in terms of seasonal water-source fluxes and uptake from the rooting zones through the use of back-calculated $\delta^{18}O_{sw}^{mod}$ values. These back calculations produce an isotopic signature that is *directly* comparable to the $\delta^{18}O$ of measured and reconstructed endmember water sources (Figure 4, Table I), which enables a dynamic analysis of how fluctuations in hydrology affect trees and forests.

The recorded sub-annual variability in $\delta^{18}O_{sw}^{mod}$ used by each species, most notably the comparison between the early- and latewood components (Figure 7b and c), provides direct information about the seasonal changes in the availability of water within both floodplain reservoirs (vadose versus phreatic) for tree growth. The restriction of *Fraxinus* rooting depth above the gravel layer limits water access to the vadose zone, and therefore to infiltrated precipitation (Singer *et al.,* 2013, 2014). The pattern of *Fraxinus* $\delta^{18}O_{sw}^{mod}$ confirms an oscillating reliance for growth on precipitation derived from the NGS and GS (Figure 4 and 8a). We identify isotopically depleted winter precipitation as the primary moisture source for earlywood *Fraxinus* growth, as it recharges upper soil layers during the non-growing season months and becomes available at the onset of the growing season. *Fraxinus* latewood, by contrast, isotopically reflects growing season precipitation modified by evaporative enrichment, although its sub-annual record of water use (both earlywood and latewood) may be occasionally punctuated by isotopically depleted rainfall events, reliance on matric bound moisture that is isotopically distinct from the cotemporary growing season rainfall (Brooks *et al.,* 2010) and phreatic water being supplied to the rooting zone of *Fraxinus* when the water table rises into the vadose zone (e.g. 2003 Figure 8a).

Forecasts of future rainfall in Mediterranean climate zones include high spatial and temporal variability (Kovats *et al.,* 2014). Furthermore, reductions in precipitation and increases in temperature are expected during the summer months (Dai, 2012; Jin *et al.,* 2010; Kovats *et al.,* 2014; Mariotti *et al.,* 2008), which would likely produce increased vulnerability of these forests to water stress (Allen *et al.,* 2010; Choat *et al.,* 2012; McDowell and Allen, 2015; Vicente-Serrano *et al.,* 2013). In this context of the impact of climate change on water availability, *Fraxinus* is considered to be a drought tolerant, capable of reducing water losses and hydraulic conductance in order to resist xylem cavitation (Lemoine *et al.,* 2001; Peltier and Marigo, 1999), which may give it a competitive advantage under future climatic conditions. However, it is unclear how it will adapt to apparently sharing vadose zone water with *Populus*.

The phreatophytic rooting of *Populus* is clearly exemplified through its depleted $\delta^{18}O_{sw}^{mod}$ values, which are comparable to hyporheic derived riverine (snowmelt) water and is consistent with prior documentation of its reliance on phreatic water (Busch *et al.,* 1992; Lambs *et al.,* 2002; Rood *et al.,* 2003; Smith *et al.,* 1991) (Figure 4, 8b and 9a). The uptake of water from the saturated zone appears to occur throughout the entire growing season (2000–2006 period), but we note that the variability in $\delta^{18}O_{sw}^{mod}$ is a likely result of differential access to a varying mix of hyporheic discharge and regional groundwater sourced water from the nearby Massif Central (Figure 9a). Our preliminary analysis suggests that the amplitude of *Populus* $\delta^{18}O_{sw}^{mod}$ depletion is driven by the timing and volume of river discharge (i.e. shape of the annual hydrograph). Indeed, the seasonal pattern of discharge may be more important than annual mean streamflow to riparian ecology (Barnett *et al.,* 2005; Greet *et al.,* 2011). Within snowmelt-dominated river basins, such as the Rhône, the timing of spring flood peaks are particularly important for *Populus* seed dispersal and seedling recruitment, and GS discharge is critical for mature trees which generally require access to the water table, supported by hyporheic flow (Rood *et al.,*

2008; Singer and Dunne, 2004). Under projected climate changes expressing as increases in temperature and reductions in precipitation, Mediterranean regions are expected to experience a shift in river regimes from that of snowmelt to runoff dominated, which would significantly impact the seasonality of streamflow (Barnett *et al.,* 2005; García-Ruiz *et al.,* 2011; Kovats *et al.,* 2014). River discharges are expected to increase during the winter as the result of a change in the partitioning of precipitation toward more rain rather than snow. This combined with a reduced snowpack under warmer spring temperatures would generate earlier snowmelt, and reduce stream water provision for GS hyporheic flow precisely when forest water demand is greatest (Barnett *et al.,* 2005; García-Ruiz *et al.,* 2011; Rood *et al.,* 2008). These changes to climatic forcing would likely have a negative effect on phreatophytes (e.g. *Populus spp*.), which are highly vulnerable to xylem cavitation, leading to reduced growth, branch die back and eventual mortality under prolonged periods of water deficit (Amlin and Rood, 2003; Bréda *et al.,* 2006; Rood *et al.,* 2008; Singer *et al.,* 2013).

Populus is opportunistic in its water acquisition strategies, capable of utilizing vadose moisture during periods of drought (Snyder and Williams, 2000) via smaller roots closer to the surface (Singer *et al.,* 2014). This water-use strategy may develop following periodic or sustained separation of its roots from the water table because of the effects of streamflow regulation and/or channel incision (Amlin and Rood, 2003). The convergence in $\delta^{18}O_{sw}^{mod}$ for both *Fraxinus* and *Populus* after 2007 suggests that *P. nigra* became disconnected from its phreatic water source, which we interpret as a decline of the near-channel floodplain water table. However, discharge data on their own do not support a reduction in streamflow. We therefore investigated whether an alternative mechanism may have led to a reduction in water table height. Channel bathymetry data for the Rhône River adjacent to our study site (Figure 10a and b) (unpublished thesis of Elsa Parrot, ENS-Lyon, 2015), shows that there was significant recent incision of the riverbed along this reach of the Rhône near our sampled trees (PK 174.5). This section of river has shown a progressive pattern of intermittent channel incision since records began. Most importantly, between 1998 and 2007 the channel incised by 2 m, and the greatest rate of riverbed down-cutting occurred between 2003 and 2007, resulting in 1.5 m of incision. Because channel elevation affects local river stage, river stage affects lateral hyporheic flow and hyporheic flow affects floodplain water table elevation, these data provide evidence that the phreatic water table declined substantially in the period leading up to 2007, perhaps crossing a threshold for separating *P. nigra* roots from the phreatic water source (e.g. Scott *et al.,* 2000). Following this decline, *Populus* evidently has relied on precipitation derived water within the vadose zone, tracking the same $\delta^{18}O_{ppt}$ utilized by *Fraxinus* at the sub-annual level. *Populus*, therefore, has apparently switched its water source to vadose zone moisture on a consistent basis, rather than transient uptake associated with periodic drought stress. Now it apparently must compete with *Fraxinus* for the same floodplain water, which may be problematic for one or both of these species in the future.

Although the separation of *Populus* roots from the water table, shown here, was apparently a consequence of channel incision, we would also expect climatically driven declines in streamflow to produce similar changes in available phreatic water (Singer *et al.,* 2013). Under projected changes in climate, riparian cottonwoods within Mediterranean biomes, particularly in snowmelt dominated basins, (i.e. Southern Europe and Northern California) could face increasing drought conditions because of water table decline (Rood *et al.,* 2008; Singer *et al.,* 2013). As these drought conditions become more frequent we could witness declines in *Populus* populations with floodplain forests becoming dominated by more drought tolerant species (e.g. *Fraxinus*).

This study has highlighted the utility of high resolution isotopic sampling of tree-rings in combination with mechanistic modelling in providing retrospective information

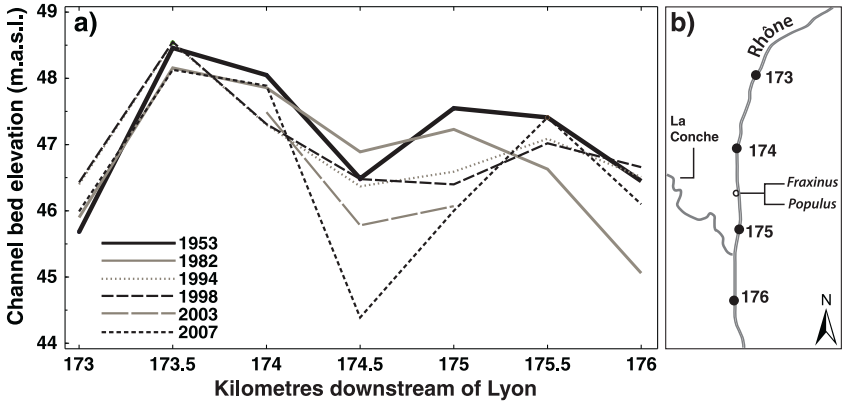

Figure 10. Channel bed elevation data of (a) the stretch of Rhône adjacent to field site and (b) sampling positions in relation to tree locations.

on the seasonal fluctuations in source water availability to riparian trees. We believe that such methods could be further enhanced through the incorporation of a dual isotope approach, utilizing $\delta^{13}C$ to uncover the historical physiological responses of riparian trees to changes in source water availability (e.g. Sarris *et al.,* 2013). Furthermore, we posit that trends in channel morphology (Slater and Singer, 2013; Slater *et al.,* 2015), as well as within site heterogeneity in hydro-geomorphic characteristics may prove to be important controls on the seasonal availability of water sources for tree growth (Singer *et al.,* 2014), which should be a focus of future research.

CONCLUSION

In this paper we demonstrated a new set of methods for investigating the historical water source used by two co-occurring riparian trees throughout the growing season. We micro-sliced individual tree rings, analysed them for $\delta^{18}O_{cell}$ and inversely modelled the source water used for the growth of each micro-slice. In order to assess the history of hydrological partitioning, we compared the $\delta^{18}O$ results from the micro-slices with endmember analyses of sampled waters, as well as against detailed time series of key hydrological variables. We showed how the seasonal water availability varied for each species as a function of their rooting depths. This allowed us to distinguish between the different water sources involved in floodplain hydrological partitioning and supplying moisture for tree growth during different parts of the growing season. We identified seasonal patterns in water use that generally reflect winter precipitation followed by growing season precipitation $\delta^{18}O$ (*Fraxinus*) and Massif Central-derived phreatic water followed by Rhône River phreatic water (*Populus*). We also note that water sources for these two species converged from 2007 to 2010, suggesting a loss of access to phreatic water for *Populus*, and therefore potentially increased competition with *Fraxinus* for a limited vadose zone water source. We suggest that the nature of these results is not unique to riparian forests of the Rhône, but could represent more general patterns to be expected in water-stressed Mediterranean biomes, particularly under a climate projected to become warmer and drier. We believe the set of methods outlined here could improve efforts to hindcast past floodplain hydrological partitioning and plant-water relations, as well as to improve predictions of tree and forest response to future climate changes.

ACKNOWLEDGEMENTS

This work was supported finacially by a Natural Environment Research Council studentship to CIS, Observatoire Hommes/Milieux Vallée du Rhône and the Department of Earth and Environmental Sciences at the University of St Andrews. We thank Cheryl Wood and Angus Calder for laboratory assistance and advice, Cristina Evans for help coding the inverse Barbour model, Carol and Tony Sargeant, Rory McDonald and Thomas Smith for field assistance and Hervé Piegay for consultation and provision of channel bathymetric data.

REFERENCES

Alaghmand S, Beecham S, Jolly ID, Holland KL, Woods JA, Hassanli A. 2014. Modelling the impacts of river stage manipulation on a complex river–floodplain system in a semi-arid region. *Environmental Modelling & Software* **59**: 109–126.

Allen CD, Macalady AK, Chenchouni H, Bachelet D, McDowell N, Vennetier M, Kitzberger T, Rigling A, Breshears DD, Hogg ET, Gonzalez P. 2010. A global overview of drought and heat-induced tree mortality reveals emerging climate change risks for forests. *Forest Ecology and Management* **259**(4): 660–684.

Alstad KP, Hart SC, Horton JL, Kolb TE. 2008. Application of tree-ring isotopic analyses to reconstruct historical water use of riparian trees. *Ecological Applications* **18**(2): 421–437.

Amlin NM, Rood SB. 2002. Comparative tolerances of riparian willows and cottonwoods to water-table decline. *Wetlands* **22**(2): 338–346.

Amlin N, Rood S. 2003. Drought stress and recovery of riparian cottonwoods due to water table alteration along Willow Creek, Alberta. *Trees* **17**: 351–358.

Barbour MM, Roden JS, Farquhar GD, Ehleringer JR. 2004. Expressing leaf water and cellulose oxygen isotope ratios as enrichment above source water reveals evidence of a Péclet effect. *Oecologia* **138**(3): 426–435.

Barbour MM, Walcroft AS, Farquhar GD. 2002. Seasonal variation in $\delta^{13}C$ and $\delta^{18}O$ of cellulose from growth rings of *Pinus radiata*. *Plant, Cell and Environment* **25**(11): 1483–1499.

Barnett TP, Adam JC, Lettenmaier DP. 2005. Potential impacts of a warming climate on water availability in snow-dominated regions. *Nature* **438**(7066): 303–309.

Berkelhammer M, Stott LD. 2009. Modeled and observed intra-ring δ18O cycles within late Holocene Bristlecone Pine tree samples. *Chemical Geology* **264**(1–4): 13–23.

Boé J, Terray L, Martin E, Habets F. 2009. Projected changes in components of the hydrological cycle in French river basins during the 21st century. *Water Resources Research* **45**(8).

Bowen GJ, Wilkinson B. 2002. Spatial distribution of δ18O in meteoric precipitation. *Geology* **30**(4): 315–318.

Bowen GJ, Wassenaar LI, Hobson KA. 2005. Global application of stable hydrogen and oxygen isotopes to wildlife forensics. *Oecologia* **143**: 337–348. DOI:10.1007/s00442-004-1813-y.

Bowen, GJ. 2015 The Online Isotopes in Precipitation Calculator, version 2.2. http://www.waterisotopes.org.

Bravard J-P. 2010. Discontinuities in braided patterns: the River Rhône from Geneva to the Camargue delta before river training. *Geomorphology* **117**(3–4): 219–233.

Bréda N, Huc R, Granier A, Dreyer E. 2006. Temperate forest trees and stands under severe drought: a review of ecophysiological responses, adaptation processes and long-term consequences. *Annals of Forest Science* **63**(6): 625–644.

Brookman T, Whittaker T. 2012. Experimental assessment of the purity of α-cellulose produced by variations of the Brendel method: Implications for stable isotope (δ13C, δ18O) dendroclimatology. *Geochemistry, Geophysics, Geosystems* **13**(9): 1–17.

Brooks JR, Barnard HR, Coulombe R, McDonnell JJ. 2010. Ecohydrologic separation of water between trees and streams in a Mediterranean climate. *Nature Geoscience* **3**(2): 100–104.

Busch D, Ingraham N, Smith S. 1992. Water uptake in woody riparian phreatophytes of the southwestern United States: a stable isotope study. *Ecological Applications* **2**(4): 450–459.

Celle-Jeanton H, Travi Y, Blavoux B. 2001. Isotopic typology of the precipitation in the Western Mediterranean Region at three different time scales. *Geophysical Research Letters* **28**(7): 1215–1218.

Choat B, Jansen S, Brodribb TJ, Cochard H, Delzon S, Bhaskar R, Bucci SJ, Feild TS, Gleason SM, Hacke UG, Jacobsen AL. 2012. Global convergence in the vulnerability of forests to drought. *Nature* **491**(7426): 752–755.

Craig H, Gordon L. 1965. Deuterium and oxygen-18 variations in the ocean and marine atmosphere. In *Proceedings of a conference on Stable isotopes in Oceanographic studies and Paleotemperatures, Spoleto, Italy*. pp. 9–130.

Cuny HE, Rathgeber CB, Frank D, Fonti P, Mäkinen H, Prislan P, Rossi S, del Castillo EM, Campelo F, Vavrčík H, Camarero JJ. 2015. Woody biomass production lags stem-girth increase by over one month in coniferous forests. *Nature Plants* **1**(11): 15160.

Dai A. 2012. Increasing drought under global warming in observations and models. *Nature Climate Change* **3**(1): 52–58.

Dansgaard W. 1964. Stable isotopes in precipitation. *Tellus* **16**(4): 436–468.

Dawson TE, Ehleringer JR. 1991. Streamside trees that do not use stream water. *Nature* **350**(6316): 335–337.

Delattre H, Vallet-Coulomb C, Sonzogni C. 2015. Deuterium excess in atmospheric water vapor of a Mediterranean coastal wetland: regional versus local signatures. *Atmospheric Chemistry and Physics Discussions* **15**(2): 1703–1746.

Dongmann G, Nürnberg HW, Förstel H, Wagener K. 1974. On the enrichment of H2 18O in the leaves of transpiring plants. *Radiation and Environmental Biophysics* **11**(1): 41–52.

Dufour S, Piégay H. 2008. Geomorphological controls of *Fraxinus excelsior* growth and regeneration in floodplain forests. *Ecology* **89**(1): 205–215.

Etchevers P, Golaz C, Habets F, Noilhan J. 2002. Impact of a climate change on the Rhone river catchment hydrology. *Journal of Geophysical Research: Atmospheres* **107**(D16).

Evans MN, Schrag DP. 2004. A stable isotope-based approach to tropical dendroclimatology. *Geochimica et Cosmochimica Acta* **68**(16): 3295–3305.

Flanagan LB, Ehleringer JR. 1991. Stable isotope composition of stem and leaf water: applications to the study of plant water use. *Functional Ecology* **5**(2): 270–277.

García-ruiz JM, López-Moreno JI, Vicente-Serrano SM, Lasanta-Martínez T, Beguería S. 2011. Mediterranean water resources in a global change scenario. *Earth Science Reviews* **105**(3–4): 121–139.

Gat JR. 1996. Oxygen and hydrogen isotopes in the hydrologic cycle. *Annual Review of Earth and Planetary Sciences* **24**(1): 225–262.

Gaudinski JB, Dawson TE, Quideau S, Schuur EA, Roden JS, Trumbore SE, Sandquist DR, Oh SW, Wasylishen RE. 2005. Comparative analysis of cellulose preparation techniques for use with 13 C, 14 C, and 18 O isotopic measurements. *Analytical Chemistry* **77**(22): 7212–7224.

Gazis C, Feng X. 2004. A stable isotope study of soil water: evidence for mixing and preferential flow paths. *Geoderma* **119**(1–2): 97–111.

González E, González-Sanchis M, Cabezas Á, Comín FA, Muller E. 2010. Recent changes in the riparian forest of a large regulated Mediterranean river: implications for management. *Environmental Management* **45**(4): 669–681.

Graillot D, Paran F, Déchomets R, Marmonier P, Piscart C, Simon L, Bornette G, Baillet H, Rodriguez C, Travi Y. 2010. Evaluation des échanges nappes/rivière et de la part des apports souterrains dans l'alimentation des eaux de surface (cours d'eau, plans d'eau, zones humides) Application au fleuve Rhône et aux aquifères associés Influence des variations saisonnières sur les échanges, *Rapport à l'Agence de l'eau RMC*, pp 1-148.

Greet J, Angus Webb J, Cousens RD. 2011. The importance of seasonal flow timing for riparian vegetation dynamics: a systematic review using causal criteria analysis. *Freshwater Biology* **56**(7): 1231–1247.

Hill SA, Waterhouse JS, Field EM, Switsur VR, Ap Rees T. 1995. Rapid recycling of triose phosphates in oak stem tissue. *Plant, Cell & Environment* **18**(8): 931–936.

IAEA/WMO (2015). Global network of isotopes in precipitation. The GNIP Database. Accessible at: http://www.iaea.org/water

Jean-François B. 2011. Hydrological and post-depositional impacts on the distribution of Holocene archaeological sites: the case of the Holocene middle Rhône River basin, France. *Geomorphology* **129**(3–4): 167–182.

Jin F, Kitoh A, Alpert P. 2010. Water cycle changes over the Mediterranean: a comparison study of a super-high-resolution global model with CMIP3. *Philosophical transactions. Series A, Mathematical, physical, and engineering sciences* **368**(1931): 5137–49.

Kovats RS, Valentini R, Bouwer LM, Georgopoulou E, Jacob D, Martin E, Rounsevell M, Soussana J-F. 2014. Europe. In: Climate change 2014: impacts, adaptation, and vulnerability. In *Part B: Regional Aspects. Contribution of Working Group II to the Fifth Assessment Report of the Intergovernmental Panel on Climate Change*, Barros VR, Field CB, Dokken DJ, Mastrandrea MD, Mach KJ, Bilir TE, Chatterjee M, Ebi KL, Estrada YO, Genova RC, Girma B, Kissel ES, Levy AN, MacCracken S, Mastrandrea PR, White LL (eds). Cambridge University Press: Cambridge, United Kingdom and New York, NY, USA; 1267–1326.

Lambs L, Lourdes J, Berthelot M. 2002. The use of the stable oxygen isotope (18O) to trace the distribution and uptake of water in riparian woodlands. *NUKLEONIKA* **47**(Supplement 1): 1–4.

Lambs L, Loubiat M, Girel J, Tissier J, Peltier JP, Marigo G. 2006. Survival and acclimatation of *Populus nigra* to drier conditions after damming of an alpine river, southeast France. *Annals of Forest Science* **63**(4): 377–385.

Lemoine D, Peltier J-P, Marigo G. 2001. Comparative studies of the water relationsand the hydraulic characteristics in *Fraxinus excelsior*, *Acer pseudoplatanus* and *A. opalus* trees under soil water contrasted conditions. *Annals of Forest Science* **58**(7): 723–731.

Managave SR, Sheshshayee MS, Ramesh R, Borgaonkar HP, Shah SK, Bhattacharyya A. 2011. Response of cellulose oxygen isotope values of teak trees in differing monsoon environments to monsoon rainfall. *Dendrochronologia* **29**(2): 89–97.

Mariotti A, Zeng N, Yoon JH, Artale V, Navarra A, Alpert P, Li LZ. 2008. Mediterranean water cycle changes: transition to drier 21st century conditions in observations and CMIP3 simulations. *Environmental Research Letters* **3**(4): 044001.

Marshall JD, Monserud RA. 2006. Co-occurring species differ in tree-ring 18O trends. *Tree Physiology* **26**(8): 1055–1066.

MATLAB (R2013a) (The MathWorks, Inc., Natick, Massachusetts, United States) (n.d)

McCarroll D, Loader NJ. 2004. Stable isotopes in tree rings. *Quaternary Science Reviews* **23**(7–8): 771–801.

McDowell NG, Allen CD. 2015. Darcy's law predicts widespread forest mortality under climate warming. *Nature Clim. Change* **5**(7): 669–672.

Nakatsuka T, Ohnishi K, Hara T, Sumida A, Mitsuishi D, Kurita N, Uemura S. 2004. Oxygen and carbon isotopic ratios of tree-ring cellulose in a conifer-hardwood mixed forest in northern Japan. *Geochemical Journal* **38**(1): 77–88.

NOAA (2016). Global Summary of the Day. Accessible at: https://data.noaa.gov/dataset/global-surface-summary-of-the-day-gsod

Parrot E. 2015. Analyse spatio-temporelle de la morphologie du chenal du Rhône du Léman a la Méditerranéen (PhD Thesis), ENS, Lyon: 466

Peltier J-P, Marigo G. 1999. Drought adaptation in *Fraxinus excelsior* L.: physiological basis of the elastic adjustment. *Journal of Plant Physiology* **154**(4): 529–535.

Penna D, Oliviero O, Assendelft R, Zuecco G, van Meerveld IH, Anfodillo T, Carraro V, Borga M, Dalla Fontana G. 2013. Tracing the water sources of trees and streams: isotopic analysis in a small pre-alpine catchment. *Procedia Environmental Sciences* **19**: 106–112.

Poussart PF, Schrag DP. 2005. Seasonally resolved stable isotope chronologies from northern Thailand deciduous trees. *Earth and Planetary Science Letters* **235**(3–4): 752–765.

Roden J, Lin G, Ehleringer J. 2000. A mechanistic model for interpretation of hydrogen and oxygen isotope ratios in tree-ring cellulose. *Geochimica et Cosmochimica Acta* **64**(1): 21–35.

Roden JS, Johnstone JA, Dawson TE. 2009. Intra-annual variation in the stable oxygen and carbon isotope ratios of cellulose in tree rings of coast redwood (*Sequoia sempervirens*). *The Holocene* **19**(2): 189–197.

Rood SB, Braatne JH, Hughes FMR. 2003. Ecophysiology of riparian cottonwoods: stream flow dependency, water relations and restoration. *Tree Physiology* **23**(16): 1113–1124.

Rood SB, Pan J, Gill KM, Franks CG, Samuelson GM, Shepherd A. 2008. Declining summer flows of Rocky Mountain rivers: changing seasonal hydrology and probable impacts on floodplain forests. *Journal of Hydrology* **349**: 397–410.

Sánchez-Pérez JM, Lucot E, Bariac T, Trémolières M. 2008. Water uptake by trees in a riparian hardwood forest (Rhine floodplain, France). *Hydrological Processes* **22**(3): 366–375.

Sarris D, Siegwolf R, Körner C. 2013. Inter- and intra-annual stable carbon and oxygen isotope signals in response to drought in Mediterranean pines. *Agricultural and Forest Meteorology* **168**: 59–68.

Scott ML, Lines GC, Auble GT. 2000. Channel incision and patterns of cottonwood stress and mortality along the Mojave River, California. *Journal of Arid Environments* **44**(4): 399–414.

Singer MB, Dunne T. 2004. An empirical-stochastic, event-based program for simulating inflow from a tributary network: framework and application to the Sacramento River basin, California. *Water Resources Research* **40**(7): W07506/1–W07506/14.

Singer MB, Stella JC, Dufour S, Piégay H, Wilson RJ, Johnstone L. 2013. Contrasting water-uptake and growth responses to drought in co-occurring riparian tree species. *Ecohydrology* **6**(3): 402–412.

Singer MB, Sargeant CI, Piégay H, Riquier J, Wilson RJ, Evans CM. 2014. Floodplain ecohydrology: climatic, anthropogenic, and local physical controls on partitioning of water sources to riparian trees. *Water Resources Research* **50**(5): 4490–4513.

Slater LJ, Singer MB. 2013. Imprint of climate and climate change in alluvial riverbeds: continental United States, 1950–2011. *Geology* **41**(5): 595–598.

Slater LJ, Singer MB, Kirchner JW. 2015. Hydrologic versus geomorphic drivers of trends in flood hazard. *Geophysical Research Letters* **42**(2): 370–376.

Smith SD, Wellington AB, Nachlinger JL, Fox CA. 1991. Functional responses of riparian vegetation to streamflow diversion in the Eastern Sierra Nevada. *Ecological Applications* **1**(1): 89–97.

Snyder KA, Williams DG. 2000. Water sources used by riparian trees varies among stream types on the San Pedro River, Arizona. *Agricultural and Forest Meteorology* **105**(1–3): 227–240.

Stella JC, Rodríguez-González PM, Dufour S, Bendix J. 2012. Riparian vegetation research in Mediterranean-climate regions: common patterns, ecological processes, and considerations for management. *Hydrobiologia* **719**(1): 291–315.

Stromberg JC, Patten DT. 1996. Instream flow and cottonwood growth in the eastern Sierra Nevada of California, USA. *Regulated Rivers: Research & Management* **12**(1): 1–12.

Tang K, Feng X. 2001. The effect of soil hydrology on the oxygen and hydrogen isotopic compositions of plants' source water. *Earth and Planetary Science Letters* **185**: 355–367.

Treydte K, Boda S, Graf Pannatier E, Fonti P, Frank D, Ullrich B, Saurer M, Siegwolf R, Battipaglia G, Werner W, Gessler A. 2014. Seasonal transfer of oxygen isotopes from precipitation and soil to the tree ring: source water versus needle water enrichment. *New Phytologist* **202**(3): 772–783.

Verheyden A, Helle G, Schleser GH, Dehairs F, Beeckman H, Koedam N. 2004. Annual cyclicity in high-resolution stable carbon and oxygen isotope ratios in the wood of the mangrove tree *Rhizophora mucronata*. *Plant, Cell and Environment* **27**(12): 1525–1536.

Verheyden A, Helle G, Schleser GH, Beeckman H. 2006. High-resolution carbon and oxygen isotope profiles of tropical and temperate liana species. *Schriften des Forschungszentrums Jülich Reihe Umwelt* **61**: 31–35.

Vicente-Serrano SM, Gouveia C, Camarero JJ, Beguería S, Trigo R, López-Moreno JI, Azorín-Molina C, Pasho E, Lorenzo-Lacruz J, Revuelto J, Morán-Tejeda E. 2013. Response of vegetation to drought time-scales across global land biomes. *Proceedings of the National Academy of Sciences* **110**(1): 52–57.

Williams C, Cooper D. 2005. Mechanisms of riparian cottonwood decline along regulated rivers. *Ecosystems* **8**(4): 382–395.

Williams DG, Coltrain JB, Lott M, English NB, Ehleringer JR. 2005. Oxygen isotopes in cellulose identify source water for archaeological maize in the American Southwest. *Journal of Archaeological Science* **32**(6): 931–939.

Wright WE. 2008. Statistical evidence for exchange of oxygen isotopes in holocellulose during long-term storage. *Chemical Geology* **252**(1): 102–108.

Yakir D, DeNiro MJ. 1990. Oxygen and hydrogen isotope fractionation during cellulose metabolism in *Lemna gibba* L. *Plant Physiology* **93**(1): 325–332.

SUPPORTING INFORMATION

Additional supporting information may be found in the online version of this article at the publisher's web-site.

